Colloids and Surfaces B: Biointerfaces 130 (2015) 119–125

Contents lists available at ScienceDirect

Colloids and Surfaces B: Biointerfaces

journal homepage: www.elsevier.com/locate/colsurfb

Hydroxyl radical and thermal annealing on amorphous $InGaZnO_4$ films for DNA immobilizations

Dali Sun[a,*], Hiroyasu Yamahara[b], Ryosho Nakane[c,d], Hiroaki Matsui[a,d], Hitoshi Tabata[a,d]

[a] Department of Bioengineering, The University of Tokyo, 1-3-7 Hongo, Bunkyo-ku, Tokyo 113-8656, Japan
[b] Institute of Engineering Innovations, The University of Tokyo, 1-3-7 Hongo, Bunkyo-ku, Tokyo 113-8656, Japan
[c] Institute of Innovation in International Engineering Education, The University of Tokyo, 1-3-7 Hongo, Bunkyo-ku, Tokyo 113-8656, Japan
[d] Department of Electrical Engineering and Information Systems, The University of Tokyo, 1-3-7 Hongo, Bunkyo-ku, Tokyo 113-8656, Japan

ARTICLE INFO

Article history:
Received 3 December 2014
Received in revised form 20 March 2015
Accepted 9 April 2015
Available online 18 April 2015

Keywords:
DNA immobilization
Amorphous $InGaZnO_4$
Biosensor
Fluorescence
Thermal annealing

ABSTRACT

The effect of hydroxyl radicals (OH) and thermal annealing on an amorphous $InGaZnO_4$ (aIGZO) film surface was investigated for manipulation of DNA immobilization. X-ray photoemission and fluorescence measurements were conducted to reveal the status of surface OH coverage and DNA immobilization, respectively. Systematic examinations concerning OH termination on the film surface suggested that the surface coverage of OH leveling DNA immobilization was related to the local surface potential. Furthermore, OH affinity on the aIGZO film surface was sensitive to thermal annealing. A remarkable change in surface OH coverage was observed for the film surface annealed at high temperature. This behavior was framed by a structural change from amorphous to crystalline state, which regulated DNA immobilization. These results indicate that the OH affinity on aIGZO films is dependent on structural properties such as defects. This study suggests that an amorphous structure is critical for obtaining a high OH surface coverage governing DNA immobilization, and is hence more suitable for biosensing.

1. Introduction

Transparent oxide semiconductors (TOS) such as ZnO and In_2O_3 have received much attention in sensing applications for their high flexibility and visible transparency [1–4]. In particular, the visible transparency of TOS enables optical monitoring of biological and chemical reaction dynamics occurring on film surfaces, which can be further applied to electrical detection [5,6]. Among oxide semiconductors, amorphous InGaZnO (aIGZO) has attracted considerable attention for optoelectronics, including field-effect transistors and liquid crystal displays [7,8], because of its superior electron mobility and environmental and thermal stability [9,10]. These practical properties of aIGZO show great promise for biological applications.

We have previously reported that aIGZO can be a good biosensing candidate for its high DNA absorption affinity. In addition, its high DNA affinity has been shown to be directly related to its high affinity for hydroxyl radicals (OH) on the surface [11]. Moreover, control of the oxygen atmosphere during film growth is also a critical factor for carrier tunability [10,12], and we have clarified that DNA immobilization on aIGZO films is affected by oxygen pressure during film growth, because the OH affinity on the film surface can be controlled by regulating the oxygen ambiance during film growth. Thereby, oxygen ambiance during film growth can be an operable factor to achieve DNA immobilization control. In this study, we evaluated additional controllable factors for DNA immobilization on an aIGZO thin film surface, which may be easily applied after film growth. We first examined the DNA immobilization tunability through OH treatment with various NaOH concentrations. DNA immobilization showed significant dependence on the OH concentration used in surface modification.

In addition to oxygen-ambient and OH treatment control, thermal annealing after film growth has been proposed as a method for achieving control of OH affinity on an aIGZO film surface. Thermal annealing is commonly employed to improve optical, electrical, structural, and morphological properties as a consequence of enhancement in film crystal quality [13–18]. In particular, thermal annealing on an oxide-based film is known to play an important role in reducing oxygen vacancies in the host [19]. The aIGZO film is also sensitive to thermal treatment, which improves crystallinity and reduces electron traps near the conduction band [10]. Accordingly, we expected that thermal annealing on the aIGZO

Abbreviations: ssDNA, single-stranded deoxyribonucleic acid; aIGZO, amorphous indium gallium zinc oxide; XPS, X-ray photoelectron spectroscopy.

* Corresponding author. Tel.: +81 35841 1870; fax: +81 35841 1870.
E-mail address: sundali@bioxide.t.u-tokyo.ac.jp (D. Sun).

http://dx.doi.org/10.1016/j.colsurfb.2015.04.024
0927-7765/

film would also have an influence on DNA immobilization on the film surface, similar to its effect on oxygen-ambient control. Therefore, we also investigated the role of thermal annealing on the aIGZO film surface for DNA immobilization.

Single-stranded DNA (ssDNA) immobilization was employed, because ssDNA is usually used as the primary probe for the very first step in complex biological reactions such as DNA–protein and DNA–protein–ion bindings. In these reactions, a fluorescence label is selected to identify DNA immobilized on an aIGZO film surface [20]. In addition, we employed X-ray photoelectron spectroscopy (XPS), which is a well-established surface-sensitive method for detecting OH groups present on an aIGZO film surface [21]. We evaluated the OH-attaching mechanism on aIGZO film surfaces through systematic examinations of XPS and fluorescence measurements, which further supported the relationship between DNA immobilization and thermal annealing. The manipulation methods of DNA immobilization on aIGZO film surfaces introduced in this paper will contribute to extending biosensor device research based on aIGZO films with visible transparency. This work thus provides new information concerning DNA immobilization on aIGZO film surfaces.

2. Experimental

2.1. Material and reagents

High-performance liquid chromatography-purified oligonucleotides were purchased from Sigma–Aldrich Japan (Tokyo, Japan) with the following base sequence (thrombin-binding aptamer [22]) and a FAM fluorescent label at the 5′ end: 5′-TTT TTT GGT TGG TGT GGT TGG-3′. (3-Aminopropyl) trimethoxysilane (APS), sodium hydroxide, and acetone were obtained from Wako Co. Ltd. (Tokyo, Japan). All other chemicals used, unless otherwise stated, were purchased from Wako.

2.2. Film fabrication

aIGZO films with a thickness of 200 nm were deposited on Al_2O_3 substrates using radio-frequency magnetron sputtering at room temperature of 25 °C [23,24]. Sintered $InGaZnO_4$ targets were used in an Ar–O_2-mixed atmosphere of 6×10^{-1} Pa. Thermal annealing of the aIGZO films was performed as follows. As-fabricated aIGZO films were thermally treated at different temperatures (100 °C, 300 °C, 500 °C, and 700 °C) for 6 h in air. X-ray diffraction (XRD; Rigaku, Tokyo, Japan) with Cu Kα radiation was used to examine the structural quality of the obtained films.

2.3. Surface pretreatment

The aIGZO films deposited on Al_2O_3 substrates were ultrasonically cleaned in an acetone solution for 3 min, and then washed twice in deionized (DI) water for 15 min. The rinsed films were chemically treated with NaOH solutions of different concentrations for 2 h, and were then submerged into an aqueous solution of 0.2% APS for 10 min [25]. The status of OH attached on the aIGZO film surfaces was determined from the core-level spectra of O (1*s*) from XPS equipped with a monochromatized Al Kα source and a JPS-9010MC photoelectron spectrometer (JEOL Co. Ltd., Tokyo, Japan). All spectra were calibrated using an Au $4f_{5/2}$ peak taken at 87.5 eV.

2.4. DNA denaturation and absorption

Double-stranded DNA (dsDNA) dissolved in DI water was stored at 4 °C in the dark before the experiments. ssDNA was obtained by heat treatment of a dsDNA solution at 94 °C for 5 min, followed by rapid cooling in an ice bath [26]. ssDNA solutions with different concentrations were dropped onto the pre-treated aIGZO film surfaces, and then incubated at 4 °C for 12 h with constant humidity. Finally, all films were rinsed three times in DI water and air-dried. DNA immobilization on the aIGZO film surfaces was confirmed using a fluorescence variable-mode imager (GE Co. Ltd., Tokyo, Japan).

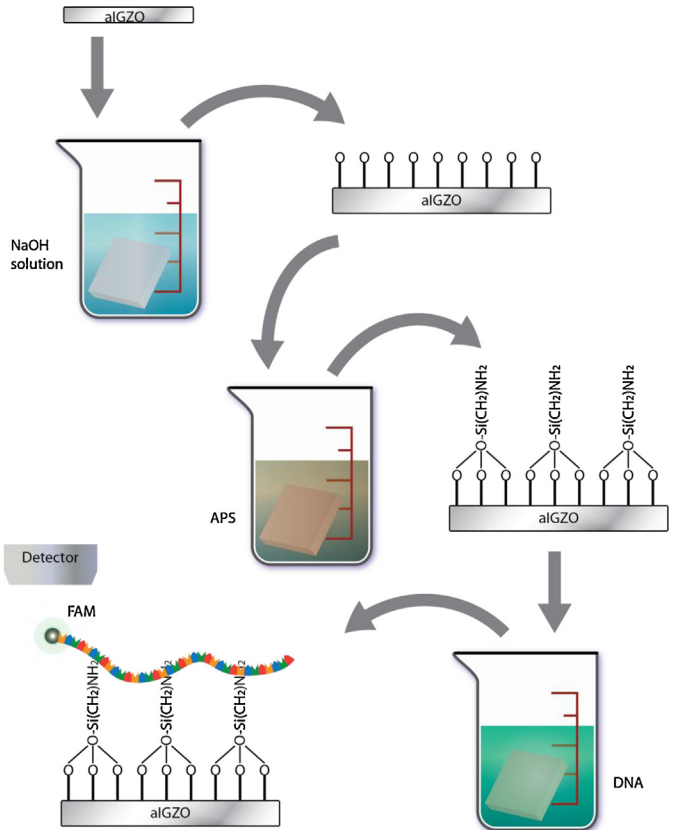

Fig. 1. Schematic figure for the immobilization process of DNA.

3. Result and discussion

3.1. Effect of OH concentration on DNA immobilization

The correlation between OH ion concentration and DNA immobilization on the aIGZO film was investigated using film samples treated with NaOH solutions at various concentrations. As shown in the scheme in Fig. 1, the aIGZO films were dipped into solutions at different NaOH concentrations for OH attachment on the film surfaces. Subsequently, APS linkers were bonded to fluorescence-labeled DNA on the basis of a physical absorption process [25]. The fluorescence label was employed as an indicator to evaluate DNA immobilization. Fig. 2 shows the correlation between fluorescence intensity and NaOH concentration. There was no significant difference in fluorescence intensity at low concentrations, below 2 mM (Fig. 2(a)), which is due to the detection limit of the florescence imager. By contrast, fluorescence intensity systematically increased with NaOH concentrations above 2 mM (Fig. 2(a) and (b)), revealing the correlation between fluorescence intensity and NaOH concentration. This result demonstrates that the OH ion concentration used in surface treatment can be a controllable factor for DNA immobilization on an aIGZO film surface. The key principle in the DNA immobilization was derived from the OH coverage efficiency on the aIGZO film surface, which is described in the following section.

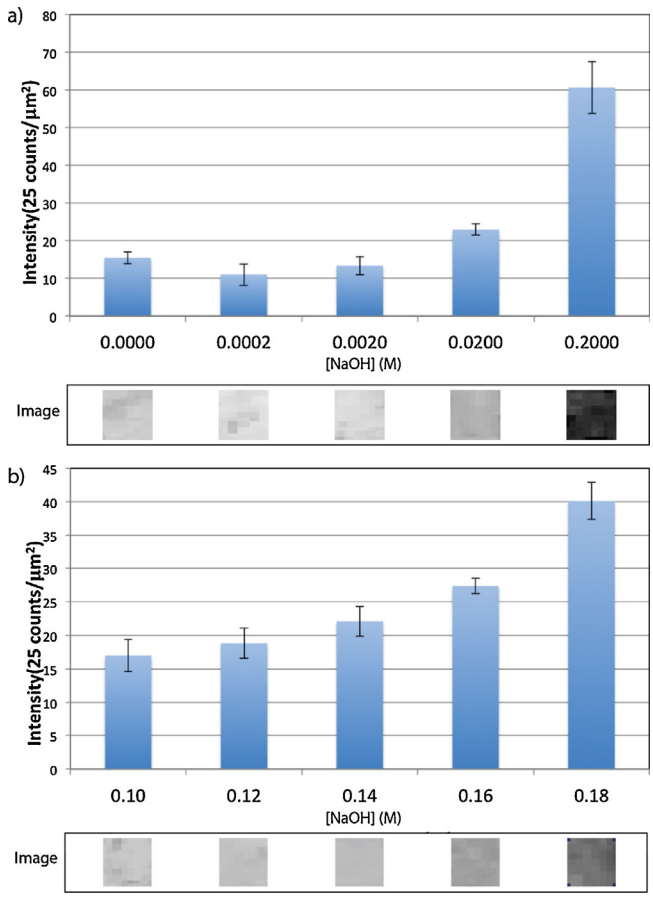

Fig. 2. Fluorescence intensity (mean ± SD, $n = 100$) and images of aIGZO films treated in NaOH solutions at various concentrations. (a) NaOH concentrations of 0 mM, 0.2 mM, 2 mM, 20 mM, and 200 mM. (b) NaOH concentrations of 100 mM, 120 mM, 140 mM, 160 mM, and 180 mM. The fluorescence intensity corresponds to 100 pixels.

3.2. Attachment of surface OH group and NaOH concentration

Alkali solutions containing OH ions have commonly been used to obtain OH-terminated surfaces [2,25]. These solutions confer the surface with OH termination to increase the surface hydrophobicity, while simultaneously extending the surface as a chemical linker for other molecules. Nevertheless, studies related to the quantitative correlation between the surface OH coverage on the film and hydroxyl concentration in the solution used for treatment are lacking. Therefore, it is indispensable to elucidate this relationship to achieve better control of surface modification.

Fig. 3 shows the XPS spectra of aIGZO film surfaces treated in solutions with different NaOH concentrations. In the core-level spectrum of O (1*s*) peak, an energy peak at around 527 eV corresponds to an oxygen ion (O^{2-}) at a divalent state, while an O (1*s*) peak at around 529 eV is attributed to an OH-related component [27–29]. In an effort to estimate the OH amount on the film surface before and after the OH treatment, we employed areas of O^{2-}- and OH-related XPS peaks that were fit with a Gaussian function. The O (1*s*) core-level spectrum was gradually dominated by the OH-related peak with increasing NaOH concentration, which was caused by the increment of surface OH coverage ($[OH]_{surface}$). The relationship between OH concentration on the film surface and the bulk solution can be expressed with the help of the Boltzmann factor [27]:

$$[OH]_{surface} = [OH]_{solution} \exp\left(\frac{e\varphi_D}{k_B T}\right) \quad (1)$$

where $[OH]_{solution}$ is the OH concentration in the solution; φ_D and T are the surface potential and temperature, respectively; e is the elementary charge (1.60218×10^{-19} C); and k_B is the Boltzmann constant (1.38066×10^{-23} J/K). This relationship is based on the mechanism that ion attachment onto a solid surface is related to the electric potential at liquid–solid interfaces, which obeys the Boltzmann statistics. Fig. 4 shows the dependence of OH-related XPS peak area (A) on NaOH concentration. The experimental data (squares in Fig. 4) could be fitted with a linear model to $\sim\exp(-e\varphi_D/k_B T)$ (dashed line in Fig. 4), which implies that the

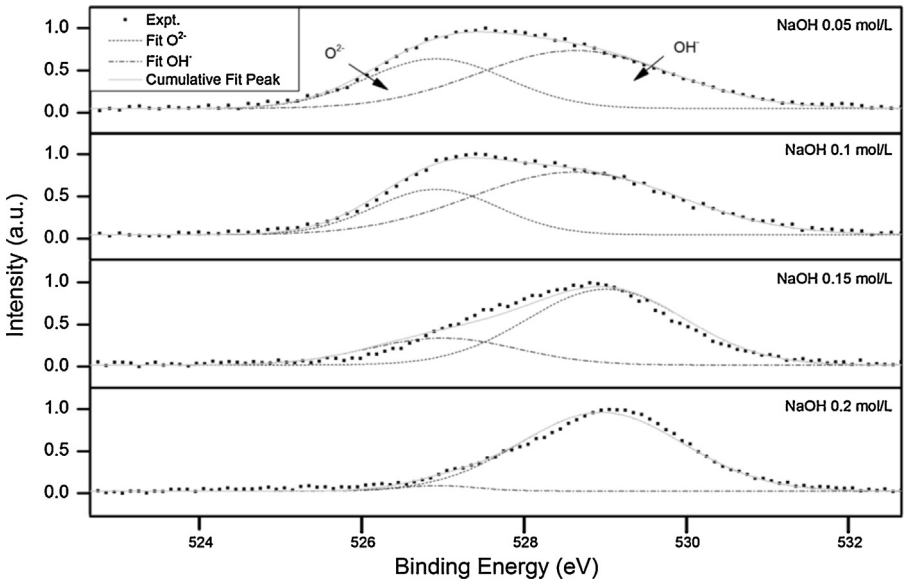

Fig. 3. Narrow XPS spectra at the O (1*s*) core-level peak on aIGZO films treated in NaOH solutions at various concentrations. The peak separation to O^{2-}- and OH-related components was achieved with a Gaussian function. Peak positions of 527 eV and 529 eV correspond to O^{2-}- and OH-related O (1*s*) components, respectively. The squares indicate raw data from XPS measurements. The short dashed lines indicate fitted curves to the O^{2-} component. The dashed dotted lines indicate fitted curves to the OH^- component. The gray solid lines indicate the cumulative fitted curves by the O^{2-} and OH^- components.

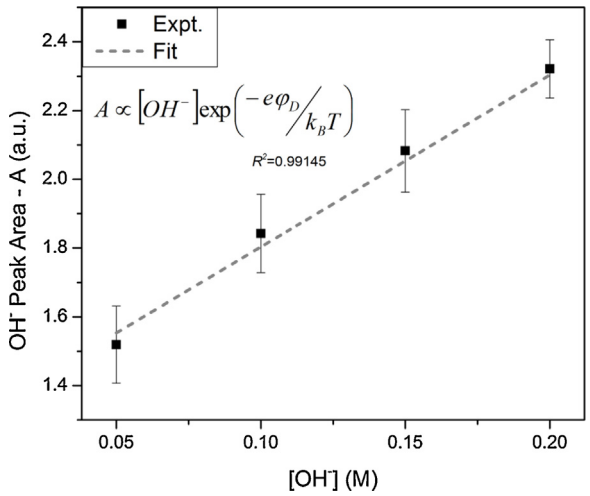

Fig. 4. Correlation between OH-related XPS peak area (A) on the film surfaces and the NaOH concentration in the solutions. The OH-related XPS peak area (A) (mean ± SD, $n = 4$) was fitted with a linear relationship to ~exp $(-e\varphi_D/k_BT)$, which can be described by Eq. (1). The squares are the means of the XPS peak area (A), and the error bars are the standard deviations. The gray dashed line indicates the result fitted to Eq. (1).

surface OH coverage on an aIGZO film is related to the electric surface potential with a φ_D value of 0.4163 V. That is, the charge balance between the aIGZO film surface and NaOH solution determines the surface OH coverage. Consequently, the electric surface potential plays a key role in controlling OH affinity on an aIGZO film surface.

3.3. Thermal annealing effect

Thermal annealing of aIGZO films for DNA immobilization was conducted under different annealing temperatures (T_a), from 100 °C to 700 °C. DNA was then immobilized on the sample surfaces following the procedure illustrated in Fig. 1. Fig. 5 shows the core-level spectrum of the O (1*s*) XPS peak for the aIGZO film surface annealed at different temperatures. At annealing temperatures of 100 °C, 300 °C, and 500 °C, all of the OH-related peaks were significantly changed after surface OH treatment with NaOH solution. This not only confirms the OH attachment on these film surfaces but also implies that annealing temperature has less influence on surface OH coverage at low annealing temperature. By contrast, the OH-related peak was essentially unshifted after the surface OH treatment at T_a = 700 °C, indicating reduced surface OH coverage upon treatment. The peak shift variance caused by annealing temperature confirms that thermal annealing is an important factor in determining OH affinity on an aIGZO film surface.

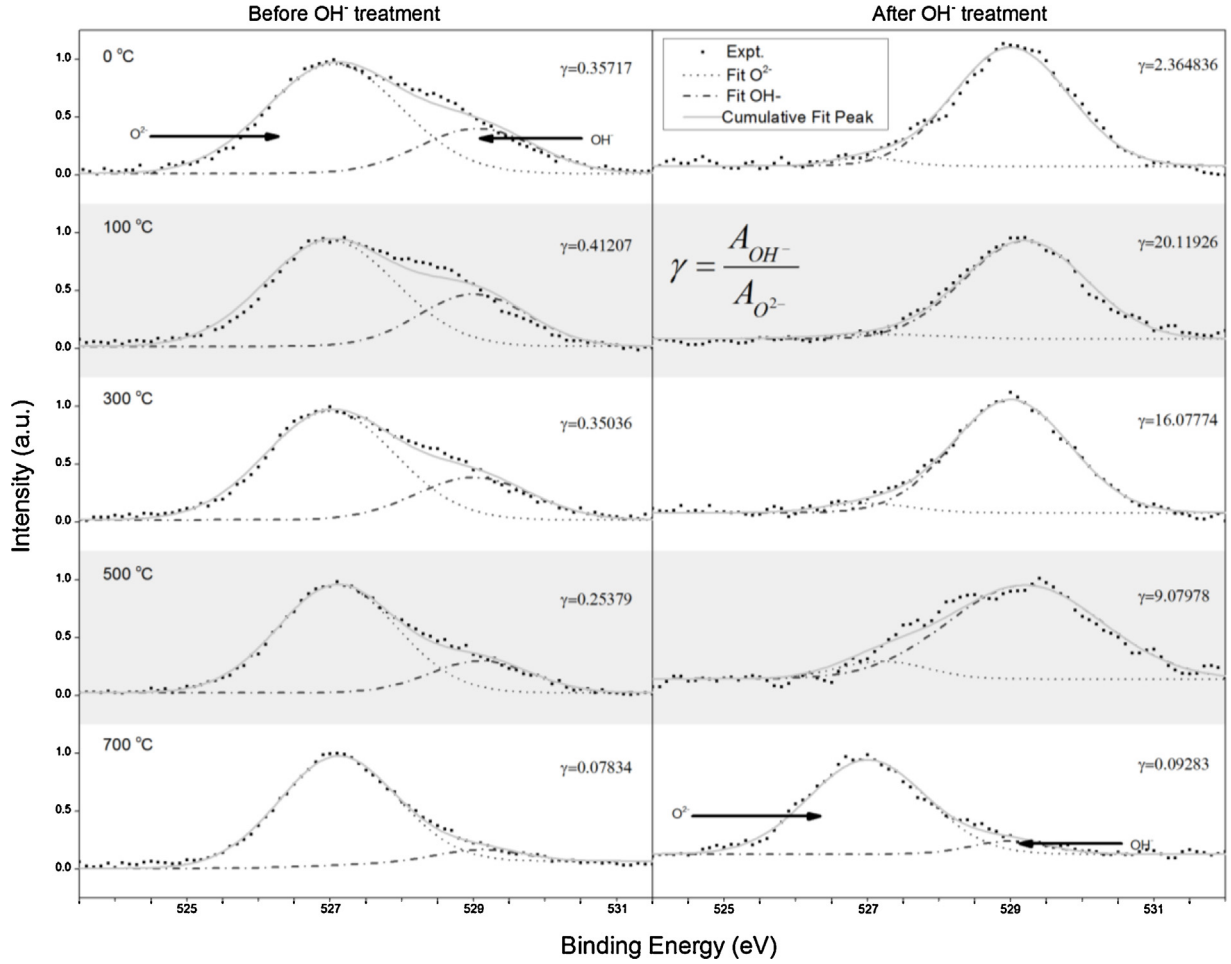

Fig. 5. Narrow XPS spectra at the O (1*s*) peak on aIGZO film surfaces as-fabricated (25 °C) and at different annealing temperatures of 100 °C, 300 °C, 500 °C, and 700 °C. The fitted peaks indicate OH^- (~529 eV) and O^{2-} (~527 eV) components. The left and right figures indicate before and after the surface treatment with NaOH, respectively. γ is defined using Eq. (2). The squares indicate raw data from XPS measurements. The short dashed lines indicate fitted curves to the O^{2-} component. The dashed dotted lines indicate fitted curves to the OH^- component. The gray solid lines indicate the cumulative fitted curve by the O^{2-} and OH^- components.

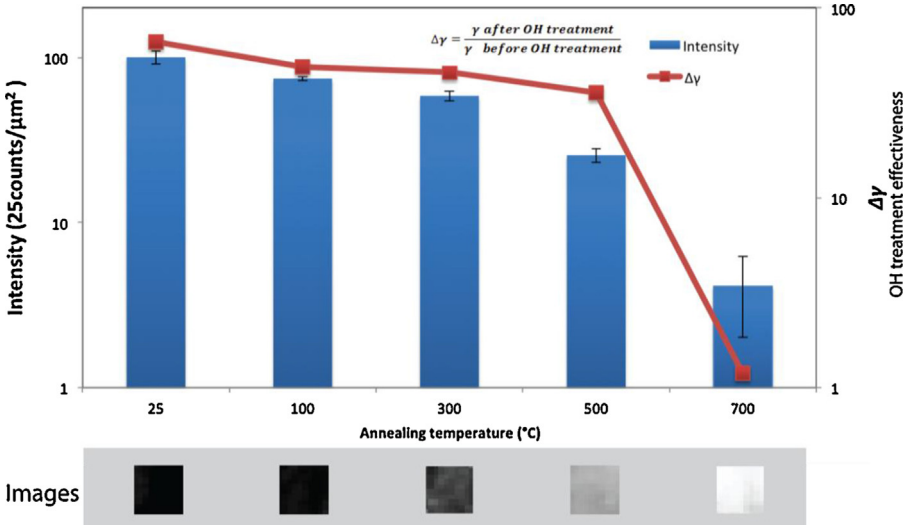

Fig. 6. Dependence of fluorescence intensity and $\Delta\gamma$ on annealing temperature. The red line ($\Delta\gamma$) is the OH treatment effectiveness defined in Eq. (3). The blue bars and error bars are the intensity means and standard deviations, respectively, obtained from the 100 pixel images shown at the bottom of the figure. (For interpretation of the references to color in this figure legend, the reader is referred to the web version of the article.)

To quantify the OH treatment effectiveness upon thermal annealing, the peak area ratio γ is defined as follows:

$$\gamma = \frac{A_{OH^-}}{A_{O^{2-}}} \quad (2)$$

where A_{OH^-} and $A_{O^{2-}}$ are the areas of OH^-- and O^{2-}-related XPS peaks, respectively. The γ values of the aIGZO thin film under various annealing temperatures before and after surface OH treatment are shown in Fig. 5. Furthermore, we define $\Delta\gamma$ as follows:

$$\Delta\gamma = \frac{\gamma \text{ afeter OH treatment}}{\gamma \text{ before OH treatment}} \quad (3)$$

where $\Delta\gamma$ represents the changing ratio of surface OH coverage upon OH treatment (OH treatment effectiveness) on an aIGZO film surface. As shown in Fig. 6, the $\Delta\gamma$ dependency on annealing temperature was similar to that observed for DNA fluorescence intensity. The maximum $\Delta\gamma$ (about 66) was observed at 25 °C, which is about 56 times higher than that observed at 700 °C (1.2). This reveals that the surface OH coverage on an aIGZO film surface is dependent on T_a, which was further reflected by the difference in DNA immobilization.

Fig. 6 also shows the dependence of fluorescence intensity on annealing temperature with DNA immobilization, which highlights the annealing effect on aIGZO films. The highest fluorescence intensity of 100 ± 9 (25 counts/μm^2) was obtained from the as-fabricated film surface at 25 °C. The fluorescence intensity slightly declined from 25 to 500 °C, but was dramatically reduced down to 4 ± 2 (25 counts/μm^2) at a high annealing temperature of 700 °C. This result demonstrated that the DNA immobilization efficiency was reduced when the annealing temperature was increased. Therefore, it is fair to assert that an aIGZO film fabricated at room temperature (25 °C) is more suitable for DNA immobilization compared to annealed films.

One possible explanation for the change in surface OH coverage observed under various annealing temperatures is an effect of crystallization in the aIGZO films. Fig. 7 shows the XRD patterns of aIGZO films annealed at different temperatures. XRD peaks for the (0 0 9) and (0 1 4) diffraction planes derived from an $InGaZnO_4$ structure were only found at a high T_a of 700 °C [8,29]. The lattice parameters of the annealed films at T_a = 700 °C were 0.285 and 2.601 nm along the *a*- and *c*-axis directions, respectively, which were slightly smaller than those of the JSPDS card (No. 038-1104). Moreover, the crystallization temperature from an amorphous to polycrystal state in aIGZO was consistent with previous reports [30,31]. Thus far, it has been reported that aIGZO films deposited at room temperature induce substantial defects in the host, contributing to the generation of electron carriers [23], which may be depressed by thermal annealing at high temperatures [30]. If the high surface OH coverage on an aIGZO film surface is related to defects on the film surface, the significant decrease in DNA immobilization observed at T_a = 700 °C (compared with that at T_a = 500 °C) may be explained by a structural change of the film sample. A similar annealing effect has been previously reported with respect to the wettability control on ZnO nanowire samples [32,33]. As discussed in Section 3.2, the surface OH coverage on an aIGZO film surface is derived from the electric surface potentials. Hence, with respect to the annealing effect, we may consider that the defects of cations and anions present on an aIGZO film surface behave as attaching sites for OH ions, which introduces a surface potential change and ultimately influences DNA immobilization.

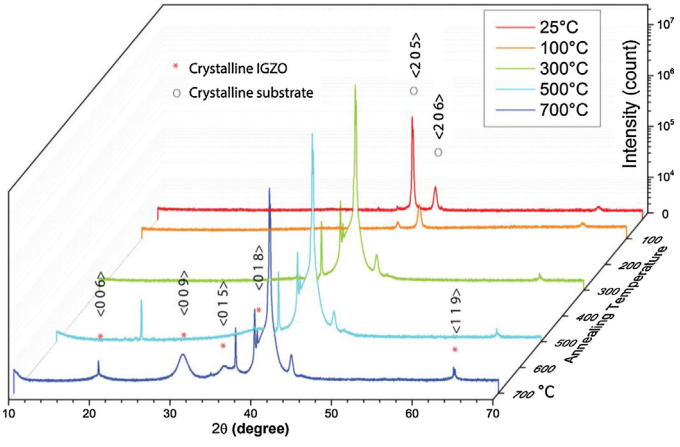

Fig. 7. XRD patterns of aIGZO films as-fabricated (25 °C, red) and annealed at different temperatures of 100 °C (orange), 300 °C (green), 500 °C (cyan), and 700 °C (blue). (For interpretation of the references to color in this figure legend, the reader is referred to the web version of the article.)

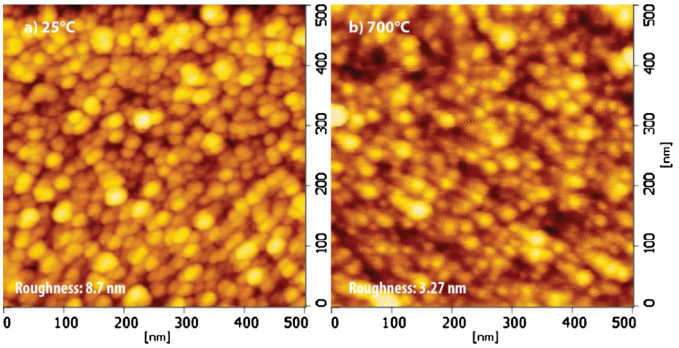

Fig. 8. AFM surface morphologies of (a) as-fabricated (25 °C) and (b) annealed aIGZO film surfaces (T_a = 700 °C).

We further evaluated the surface roughness and morphologies of the as-fabricated (at 25 °C) and annealed (T_a = 700 °C) film surfaces (Fig. 8). No remarkable difference in surface morphology was observed between the as-fabricated and annealed film surfaces. Both film surfaces were dominated by small islands of several hundred nanometers. Values of roughness on both film surfaces were in the range of several nanometers. Therefore, surface defects can be considered as the main reason for the surface OH coverage (or OH affinity) variance on the aIGZO film surfaces. The change of local electric potentials derived from surface defects of aIGZO films may primarily be responsible for the OH affinity variance on aIGZO film surfaces, which is closely linked to DNA immobilization. To prove this hypothesis, direct measurements of the surface potential on aIGZO film surfaces using Kelvin force microscopy may be necessary in future research.

4. Conclusions

We investigated the relationship between hydroxyl radicals and thermal annealing on aIGZO film surfaces for DNA immobilization. Systematic examinations using XPS and fluorescence imaging techniques revealed that DNA immobilization was strongly dependent on NaOH concentration in the solution through surface OH coverage, which can be explained using a model of electric surface potential. Furthermore, thermal annealing at the high temperature caused a structural change from the amorphous to crystal state, resulting in remarkable suppression of surface OH coverage, which suggested that OH affinity on aIGZO films was related to structural properties such as defects. Together, these results suggest that $InGaZnO_4$ in an amorphous state is more suitable for biosensing with a high DNA immobilization efficiency owing to its high OH affinity on the surface.

Acknowledgments

We are grateful to Mr. Tuguyuki Saito, Dr. Yosuke Ono, and Dr. Keiichiro Kushiro for their invaluable advice throughout the project.

References

[1] V. Stambouli, A. Zebda, E. Appert, C. Guiducci, M. Labeau, J.-P. Diard, et al., Semiconductor oxide based electrodes for the label-free electrical detection of DNA hybridization: comparison between Sb doped SnO_2 and $CdIn_2O_4$, Electrochim. Acta 51 (2006) 5206–5214, http://dx.doi.org/10.1016/j.electacta.2006.03.045
[2] A. Kaushik, P.R. Solanki, A.A. Ansari, S. Ahmad, B.D. Malhotra, A nanostructured cerium oxide film-based immunosensor for mycotoxin detection, Nanotechnology 20 (2009) 055105, http://dx.doi.org/10.1088/0957-4484/20/5/055105
[3] W. Zhang, T. Yang, D.M. Huang, K. Jiao, Electrochemical sensing of DNA immobilization and hybridization based on carbon nanotubes/nano zinc oxide/chitosan composite film, Chinese Chem. Lett. 19 (2008) 589–591, http://dx.doi.org/10.1016/j.cclet.2008.03.012
[4] K.-R. Meier, M. Grätzel, Redox targeting of oligonucleotides anchored to nanocrystalline TiO2 films for DNA detection, ChemPhysChem 3 (2002) 371–374, http://dx.doi.org/10.1002/1439-7641(20020415)3:4<371::AID-CPHC371>3.0.CO;2-O
[5] K.P. Loh, Q. Bao, G. Eda, M. Chhowalla, Graphene oxide as a chemically tunable platform for optical applications, Nat. Chem. 2 (2010) 1015–1024, http://dx.doi.org/10.1038/nchem.907
[6] M. Bras, V. Dugas, F. Bessueille, J.P. Cloarec, J.R. Martin, M. Cabrera, et al., Optimisation of a silicon/silicon dioxide substrate for a fluorescence DNA microarray, Biosens. Bioelectron. 20 (2004) 797–806, http://dx.doi.org/10.1016/j.bios.2004.03.018
[7] K. Nomura, A. Takagi, T. Kamiya, H. Ohta, M. Hirano, H. Hosono, Amorphous oxide semiconductors for high-performance flexible thin-film transistors, Jpn. J. Appl. Phys. 45 (2006) 4303–4308, http://dx.doi.org/10.1143/JJAP.45.4303
[8] M. Kim, J.H. Jeong, H.J. Lee, T.K. Ahn, H.S. Shin, J.-S. Park, et al., High mobility bottom gate InGaZnO thin film transistors with SiO[sub x] etch stopper, Appl. Phys. Lett. 90 (2007) 212114, http://dx.doi.org/10.1063/1.2742790
[9] K. Nomura, H. Ohta, A. Takagi, T. Kamiya, M. Hirano, H. Hosono, Room-temperature fabrication of transparent flexible thin-film transistors using amorphous oxide semiconductors, Nature 432 (2004) 488–492, http://dx.doi.org/10.1038/nature03090
[10] T. Kamiya, K. Nomura, H. Hosono, Origins of high mobility and low operation voltage of amorphous oxide TFTs: electronic structure, electron transport, defects and doping, J. Disp. Technol. 5 (2009) 468–483, http://dx.doi.org/10.1109/JDT. 2009.2034559
[11] D. Sun, H. Matsui, C.-N. Wu, H. Tabata, Surface treatment on amorphous $InGaZnO_4$ thin film for single-stranded DNA biosensing, Appl. Surf. Sci. 324 (2015) 310–318, http://dx.doi.org/10.1016/j.apsusc.2014.10.115
[12] M. Kimura, T. Kamiya, T. Nakanishi, K. Nomura, H. Hosono, Intrinsic carrier mobility in amorphous In–Ga–Zn–O thin-film transistors determined by combined field-effect technique, Appl. Phys. Lett. 96 (2010) 262105, http://dx.doi.org/10.1063/1.3455072
[13] G. Eftekhari, Electrical conduction in rapidly annealed sputter-deposited SiO, films (in O_2—Ar atmosphere) on Si, Phys. Status Sol. 129 (1995) 129–133.
[14] H.Q. Le, S.J. Chua, Y.W. Koh, K.P. Loh, Z. Chen, C.V. Thompson, et al., Growth of single crystal ZnO nanorods on GaN using an aqueous solution method, Appl. Phys. Lett. 87 (2005) 101908, http://dx.doi.org/10.1063/1.2041833
[15] G.C. Turner, Zinc Oxide MESFET Transistors (dissertation), University of Canterbury, Canterbury, 2009.
[16] W.J. Choi, E.J. Lee, K.S. Yoon, J.Y. Yang, J.H. Lee, C.O. Kim, et al., Annealing effects of HfO_2 gate thin films formed by inductively coupled sputtering technique at room temperature, J. Korean Phys. Soc. 45 (2004) 716–719.
[17] S.J. Xu, X.C. Wang, S.J. Chua, C.H. Wang, W.J. Fan, J. Jiang, et al., Effects of rapid thermal annealing on structure and luminescence of self-assembled InAs/GaAs quantum dots, Appl. Phys. Lett. 72 (1998) 3335, http://dx.doi.org/10.1063/1.121595
[18] G. Korotcenkov, V. Brinzari, M. Ivanov, A. Cerneavschi, J. Rodriguez, A. Cirera, et al., Structural stability of indium oxide films deposited by spray pyrolysis during thermal annealing, Thin Solid Films 479 (2005) 38–51, http://dx.doi.org/10.1016/j.tsf.2004.11.107
[19] H. Schliwinski, U. Schnakenberg, W. Windbracke, F. Mikrostrukturtechnik, D. Berlin, Thermal annealing effects on the mechanical properties of plasma-enhanced chemical vapor deposited silicon oxide films, J. Electrochem. Soc. 139 (2000) 1730–1735.
[20] J. Chen, S. Sun, C.-Z. Li, Y.-G. Zhu, B.P. Rosen, Biosensor for organoarsenical herbicides and growth promoters, Environ. Sci. Technol. 48 (2014) 1141–1147, http://dx.doi.org/10.1021/es4038319
[21] E. Mcca, J.P. Wightman, Determination of the concentration of surface hydroxyl groups on metal oxide films by a quantitative XPS method, Surf. Interface Anal. 564 (1998) 549–564.
[22] H. Cai, T.M.-H. Lee, I.-M. Hsing, Label-free protein recognition using an aptamer-based impedance measurement assay, Sens. Actuators B: Chem. 114 (2006) 433–437, http://dx.doi.org/10.1016/j.snb.2005.06.017
[23] H. Yabuta, M. Sano, K. Abe, T. Aiba, T. Den, H. Kumomi, et al., High-mobility thin-film transistor with amorphous InGaZnO[sub 4] channel fabricated by room temperature rf-magnetron sputtering, Appl. Phys. Lett. 89 (2006) 112123, http://dx.doi.org/10.1063/1.2353811
[24] K. Jeon, C. Kim, I. Song, J. Park, S. Kim, S. Kim, et al., Modeling of amorphous InGaZnO thin-film transistors based on the density of states extracted from the optical response of capacitance-voltage characteristics, Appl. Phys. Lett. 182102 (2012) 1–4, http://dx.doi.org/10.1063/1.3013842
[25] J. Xu, J. Zhu, Q. Huang, H. Chen, A novel DNA-modified indium tin oxide electrode, Electrochem. Commun. 3 (2001) 665–669.
[26] M.E. Napier, C.R. Loomis, M.F. Sistare, J.a. Kim, E. Eckhardt, H.H. Thorp, Probing biomolecule recognition with electron transfer: electrochemical sensors for DNA hybridization, Bioconjug. Chem. 8 (1997) 906–913, http://dx.doi.org/10.1021/bc9701149
[27] B. Erdem, R. Hunsicker, G. Simmons, XPS and FTIR surface characterization of TiO_2 particles used in polymer encapsulation, Langmuir 17 (2001) 2664–2669.
[28] I. Kojima, B. Li, T. Fujimoto, XRR and XPS studies of SiO_2 thin films formed by r.f. magnetron sputtering, Surf. Interface Anal. 270 (1999) 267–270.
[29] K. Shimizu, C. Phanopoulos, R. Loenders, M.-L. Abel, J.F. Watts, The characterization of the interfacial interaction between polymeric methylene diphenyl

diisocyanate and aluminum: a ToF-SIMS and XPS study, Surf. Interface Anal. 42 (2010) 1432–1444, http://dx.doi.org/10.1002/sia.3586
[30] K. Ide, K. Nomura, H. Hiramatsu, T. Kamiya, H. Hosono, Structural relaxation in amorphous oxide semiconductor, a-In-Ga-Zn-O, J. Appl. Phys. 111 (2012) 073513, http://dx.doi.org/10.1063/1.3699372
[31] K. Umeda, K. Higashi, M. Nomoto, H. Hirai, Fabrication of solution-processed oxide thin film transistors, FUJIFILM Res. Dev. 58 (2013) 60–64.
[32] X.Q. Meng, D.X. Zhao, J.Y. Zhang, D.Z. Shen, Y.M. Lu, L. Dong, et al., Wettability conversion on ZnO nanowire arrays surface modified by oxygen plasma treatment and annealing, Chem. Phys. Lett. 413 (2005) 450–453, http://dx.doi.org/10.1016/j.cplett.2005.08.039
[33] G. Li, T. Chen, B. Yan, Y. Ma, Z. Zhang, T. Yu, et al., Tunable wettability in surface-modified ZnO-based hierarchical nanostructures, Appl. Phys. Lett. 92 (2008) 173104, http://dx.doi.org/10.1063/1.2918447.